Penerbit Akademia Baru

Journal of Advanced Research in Experimental Fluid Mechanics and Heat Transfer

Journal homepage:
http://www.akademiabaru.com/submit/index.php/arefmht
ISSN: 2756-8202

Design and Fabrication of a Small Open Anechoic Wind Tunnel: Part 1

Rose Matheo Maxence[1], Yasmine El Malyani[1], Mohamed Sukri Mat Ali[2,*], Aminudin Abu[3], Mohammad Naqiuddin Nadzri[2], Muhammad Imran Firdaus Kamardan[2]

[1] Institute Technical D'ing´enieurs De L'industrie Normandie, Campus de l'Espace 1 avenue Hubert Curien CS 30802, 27200 Vernon, France
[2] Wind Engineering Laboratory, Malaysia-Japan International Institute of Technology, Universiti Teknologi Malaysia, 54100 Kuala Lumpur, Malaysia
[3] Intelligent Dynamics & System (IDS) i-Kohza, Malaysia-Japan International Institute of Technology, Universiti Teknologi Malaysia, 54100 Kuala Lumpur, Malaysia

ARTICLE INFO

Article history:
Received 22 March 2025
Received in revised form 11 April 2025
Accepted 11 May 2025
Available online 30 June 2025

Keywords:
Anechoic; wind tunnel; aeroacoustics

ABSTRACT

Anechoic wind tunnels are essential for studying aerodynamic noise, but their small-scale design poses challenges in balancing acoustic performance, flow quality and cost. This study presents the development and validation of a compact open-jet anechoic wind tunnel (2.5 m × 2.5 m × 2.5 m) with multi-layered sound-absorbing walls. The chamber's acoustic performance was evaluated through sound uniformity tests and aerodynamic noise measurements using a G.R.A.S. 40PH free-field microphone. Results confirmed effective suppression of reflections above 500 Hz, with sound pressure levels showing <5 dB variation across measurement points. The tunnel demonstrated strong mid-to-high frequency (1–10 kHz) absorption, critical for airfoil trailing-edge and turbulence noise studies. However, low-frequency (100–500 Hz) performance indicated minor non-uniformities, suggesting opportunities for improved damping. Aerodynamic noise followed a power-law scaling ($P \propto U^{2.91}$), revealing structural vibrations as a secondary noise source alongside flow-induced noise. The design met ISO 3745 standards for free-field conditions while maintaining turbulence intensities below 0.2%, suitable for fundamental aeroacoustics research. Key innovations included optimized wedge-type absorbers and a modular construction approach, enabling cost-effective replication. The study provides a validated framework for small-scale anechoic wind tunnels, addressing gaps in affordable, precision aeroacoustics testing infrastructure. Future work should target enhanced low-frequency absorption and vibration isolation to expand operational bandwidth.

1. Introduction

Anechoic wind tunnels are essential tools in aeroacoustics research, providing controlled environments for the study of noise generation and sound propagation from aerodynamic sources. Unlike traditional wind tunnels, which are typically used for aerodynamic performance testing, anechoic wind tunnels are designed to eliminate sound reflections from the walls, floor and ceiling, thus simulating a free-field condition. These specialized facilities are crucial in fields such as aircraft

* *Corresponding author.*
E-mail address: sukri.kl@utm.my (Mohamed Sukri Mat Ali)

https://doi.org/10.37934/arefmht.20.1.121135

design, automotive engineering and environmental noise control, where understanding noise emissions is as important as measuring aerodynamic forces [1-3].

The primary function of an anechoic wind tunnel is to provide a low- reflection acoustic environment, allowing for accurate noise measurements without interference from reflections. To achieve this, the walls of the test section and surrounding chamber are typically lined with sound-absorbing materials. In general, the chamber should meet international standards such as ISO 3745:2012 [4], which specifies precision methods for determining sound power levels of noise sources in anechoic and hemi-anechoic rooms. The chamber should also comply with ISO 26101:2012 [5], which defines the criteria for free-field environments necessary for accurate noise measurements [6,7].

Despite the importance of such facilities, the design and construction of anechoic wind tunnels, especially small-scale versions, present unique challenges. Large anechoic wind tunnels, such as the NASA Langley 14- by 22-Foot Subsonic Tunnel, are well-known for their complex acoustic treatments and size, allowing for high-speed airflow and precise aeroacoustic measurements [8]. However, smaller wind tunnels, designed for laboratory-scale or university research, must strike a balance between maintaining low noise levels, ensuring an adequate aerodynamic test environment and optimizing construction costs. For example, Delft University's small-scale Open Jet Facility (OJF) employs an anechoic chamber of approximately 3 m × 3 m × 3 m, capable of handling low-speed airflow and aeroacoustic measurements [9]. These smaller designs prioritize free-field acoustic conditions while accommodating limited budgets and spatial constraints, making them comparable to the wind tunnel presented in this work.

This paper presents the design, fabrication and validation of a small open anechoic wind tunnel. The test section is housed inside a custom-built anechoic chamber measuring 2.5m × 2.5m × 2.5m, optimized for low- speed aerodynamics and aeroacoustics. The chamber incorporates multi- layered sound-absorbing materials following ISO 354:2003 [10-12] standards for acoustic absorption, ensuring that noise reflections are minimized and that free-field conditions are met inside the chamber. The system was designed to provide a background noise level below 10 dB(A), making it suitable for precision measurements of low-noise aerodynamic systems.

The objective of the wind tunnel design is twofold:

i. to provide a small- scale, cost-effective platform for aeroacoustic testing in a controlled, low-noise environment
ii. to ensure that the wind tunnel meets the requirements of ISO standards for free-field conditions and noise measurement.

The chamber's performance will be validated through sound measurements using a G.R.A.S. 40PH free-field array microphone, which is compliant with IEC 61672-1:2013 standards [13,14], ensuring accurate sound pressure level (SPL) readings across a wide frequency range.

For a wind tunnel to be useful in aeroacoustic measurements, the noise from the tunnel itself must be well below the noise generated by the test object [15]. Background noise is typically generated by the blower or fan system, turbulent flow in the settling chamber and test section and structural vibrations. In anechoic wind tunnels, particular attention must be paid to the design of the blower and the use of silencers [16]. Also, problems due to blower noise could be magnified when large contraction ratios are used because the contraction acts like a horn. Therefore, contraction ratios of between about 6 - 9 are normally used [17].

The anechoic nature of a wind tunnel refers to its ability to absorb sound and prevent reflections within the test section [18]. Wedge-shaped foam absorbers, made from high-density polyurethane

or fiberglass, are typically used to line the walls of the test section. These wedges are designed to absorb sound waves over a wide range of frequencies, creating a ”free-field” condition where no sound reflections interfere with the measurements [19]. Properly designed anechoic wind tunnels should achieve absorption across frequencies relevant to aeroacoustic research, generally ranging from 200 Hz to 20 kHz [20].

In addition to acoustic treatment, an anechoic wind tunnel must also provide a stable, low-turbulence flow. High turbulence can lead to noise generation from boundary layers and flow separation, which can contaminate aeroacoustic measurements. The design of the nozzle, flow straighteners and diffusers play a key role in achieving a turbulence intensity below 0.2%, which is typical for high-quality aeroacoustic testing facilities [21].

However, most existing studies focus on large-scale anechoic tunnels, leaving a gap in optimized designs for compact, cost-effective systems suitable for laboratory or academic research. Small-scale tunnels face unique challenges, such as limited space for acoustic treatment and higher susceptibility to structural vibrations, which can distort noise measurements. This study addresses these gaps by presenting a meticulously designed small open-jet anechoic wind tunnel that balances acoustic performance, aerodynamic stability and affordability. The significance of this work lies in its potential to democratize high-quality aeroacoustic research, enabling institutions with limited resources to conduct precise noise measurements. By validating the tunnel’s performance against ISO standards and characterizing its frequency response, this study provides a replicable framework for small-scale anechoic wind tunnel design, filling a critical need in experimental aeroacoustics.

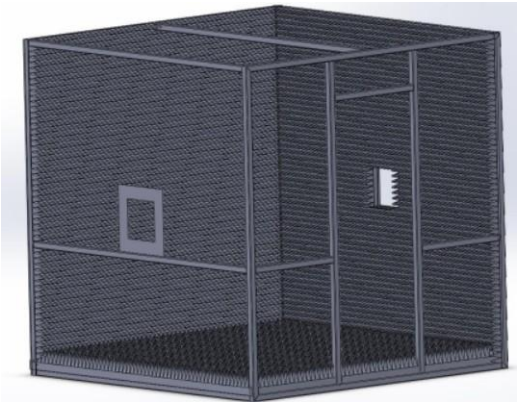

Fig. 1. Sketch of the anechoic chamber. The size of the chamber is 2.5m × 2.5m × 2.5m

2. Methodology

2.1 Anechoic Chamber Design

Figure 1 illustrates the anechoic chamber constructed for aeroacoustic investigation. The chamber is a fully enclosed structure with external dimensions of 2.5 m × 2.5 m × 2.5 m, providing sufficient space for small-scale aeroacoustic experiments:

$$V_{chamber} = 2.5^3 = 15.625\ m^3 \quad (1)$$

However, for accurate aeroacoustic measurements in an anechoic wind tunnel, it is essential that the test object is sufficiently separated from the walls to maintain free-field conditions. Guidelines from standards ISO 3745:2012 and ISO 26101:2017 emphasize the need for minimizing reflections,

which typically necessitates that the object occupies only a small fraction (often less than 10-15%) of the total chamber volume. Thus, for a chamber of 15.625 m^3, keeping the object volume to about 10-15% (≈ 1.56 to 2.34 m3) is recommended.

The walls of the chamber are treated using a multi-layered design to ensure optimal sound insulation and absorption. As depicted in Figure 2, the wall layers consist of an inner layer of 9 mm plywood that provides structural integrity. A 50 mm rockwool layer, is included for its excellent sound absorption properties. Rockwool helps to dissipate acoustic energy across a broad frequency range, minimizing the reflection of sound waves inside the chamber. A second layer of 9 mm plywood, is added as structural support while also contributing to the sound barrier. The outermost layer is 90 mm acoustic foam, designed specifically to attenuate high-frequency noise and further reduce external sound from entering the chamber. The combination of these layers provides both structural stability and sound attenuation, creating an environment suitable for aeroacoustic testing. The walls are designed to absorb noise across a wide frequency range, particularly those relevant to the noise generated in wind tunnel experiments.

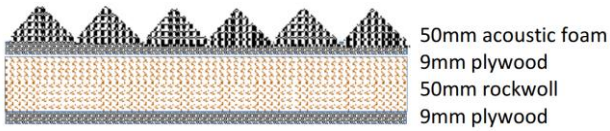

Fig. 2. Absorption material

The chamber is also equipped with acoustic wedges on the interior walls, which are designed to absorb incident sound waves and prevent their reflection back into the test section. This is crucial for ensuring that sound measurements taken during wind tunnel experiments are free from interference caused by reflected noise.

2.2 Noise Measurement Instrumentation: Free-Field Microphone

Figure 3 shows the G.R.A.S. 40PH free-field array microphone, used for precise noise measurements inside the anechoic wind tunnel chamber. This microphone is specifically designed for free-field measurements, meaning it captures sound pressure levels as they exist in a sound field without interference from reflections, making it ideal for use in anechoic environments.

Fig. 3. G.R.A.S. 40PH free-field array microphone used for noise measurements in the anechoic wind tunnel chamber

The G.R.A.S. 40PH is a precision condenser microphone that offers a broad frequency response and high sensitivity, making it suitable for detailed noise analysis in the test chamber. Its small size and omnidirectional characteristics ensure that it captures sound accurately from all directions, providing a reliable measurement of the free-field conditions within the chamber.

Key specifications of the G.R.A.S. 40PH include:

i. Frequency Range: 10 Hz to 20 kHz, which covers the full audible range of frequencies that may be generated in the wind tunnel.
ii. Dynamic Range: 18 dB(A) to 138 dB, allowing for accurate measurement of both low-level background noise and higher intensity noise sources.
iii. Free-field Calibration: Calibrated for free-field measurements, ensuring that the microphone accurately captures the noise levels without distortion from sound reflections or standing waves.
iv. IEC Compliance: The microphone is compliant with the IEC 61094-4 standard for measurement microphones [22], ensuring reliable performance in acoustic testing environments.

The noise measurements performed in the wind tunnel chamber using the G.R.A.S. 40PH microphone are conducted in accordance with ISO 3745:2012 [4], which specifies requirements for anechoic and hemi-anechoic chambers for determining the sound power levels of noise sources. Additionally, ISO 26101:2017 [5] provides guidelines for measuring noise in small enclosed spaces like the chamber used in this setup. The G.R.A.S. 40PH microphone meets the performance requirements outlined in these standards.

Figure 4 illustrates the layout of the noise measurement setup inside the small open anechoic wind tunnel. The wind tunnel test section is fully enclosed within the anechoic chamber, ensuring minimal reflections and external noise interference during the experiments. The noise source is located at the centre of the anechoic chamber and measurements are conducted at six distinct positions within the chamber, marked as Position 1 through Position 6.

The positions for noise measurement are distributed strategically within the test section to capture sound pressure levels at various locations. A common guideline is to leave a clearance of at least 0.5 m between the object and any wall. It is important to note that these calculations assume that a 0.5 m clearance is sufficient to maintain the anechoic (free-field) conditions. In practice, the required clearance may depend on the wavelengths of interest (e.g., for low-frequency measurements, a larger clearance might be necessary).

The test procedure follows these steps:

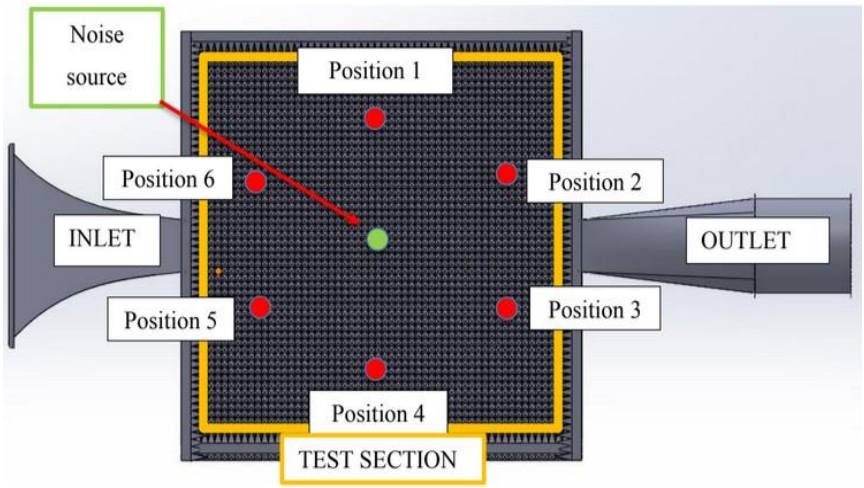

Fig. 4. Noise measurement positions inside the anechoic wind tunnel chamber. Noise measurements are performed at six positions, as indicated by the red dots, with the noise source placed near the inlet

i. Sound Source Placement: The speaker is positioned at the noise source location, centre of the anechoic wind tunnel.
ii. Sound Level Adjustments: The speaker emits sound at different frequency levels, typically ranging from 500 Hz to 10000 Hz, across three different flow speed.
iii. Noise Measurements: The sound pressure levels are recorded at each of the six positions inside the chamber. The measurements focus on the attenuation characteristics of the chamber and the uniformity of sound levels across different locations.

The goal of these measurements is to validate the chamber's ability to maintain free-field conditions and ensure that the wind tunnel operates within an acceptable noise range for aeroacoustic experiments. By comparing the measured sound levels at various positions, we can assess the chamber's performance in terms of noise reduction and identify any areas where improvements may be needed.

3. Results and Discussion

3.1 Sound Uniformity in Anechoic Chamber Design

Sound uniformity is a critical factor in the design of anechoic chambers, particularly for applications requiring precise acoustic measurements. In an ideal anechoic chamber, the sound field is uniform; that is, the sound pressure level (SPL) remains consistent across the measurement region. This uniformity is essential for several reasons. Uniform sound fields ensure that acoustic measurements are independent of the sensor location within the chamber. This consistency is crucial for obtaining accurate and reproducible results. International standards such as ISO 3745:2012 and ISO 26101:2017 specify the requirements for anechoic or semi-anechoic rooms. These standards mandate that the sound field be as uniform as possible to simulate a free-field environment. Non-uniformities in the sound field often indicate the presence of unwanted reflections or standing waves, which can distort measurements. Thus, sound measurement at six different points around the sound source have been compared.

Figure 5 presents the sound pressure fluctuations measured at six different positions inside the anechoic wind tunnel, as indicated previously in Figure 4. Each subfigure compares measurements at

two positions. In Figure 5(a), the sound pressure levels (SPL) at Position 1 and Position 4 are 85.2 dB and 89.1 dB, respectively. In Figure 5(b), the SPL values at Position 2 and Position 5 are 91.8 dB and 90.8 dB, respectively. In Figure 5(c), the SPL values at Position 3 and Position 6 are 98.8 dB and 85.5 dB, respectively.

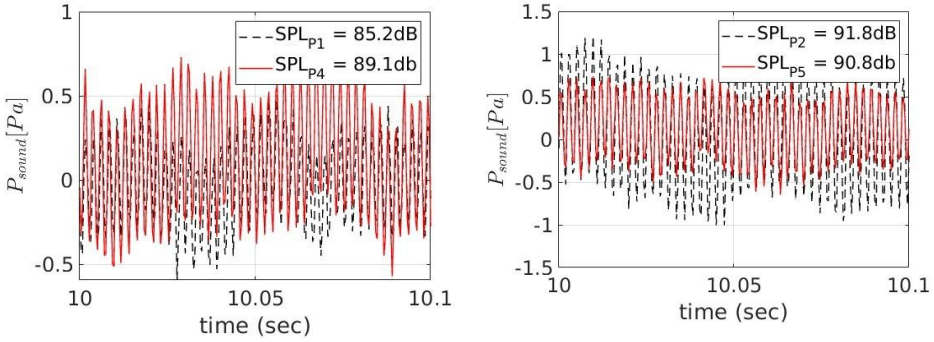

(a) Point 1 and point 4

(b) Point 2 and point 5

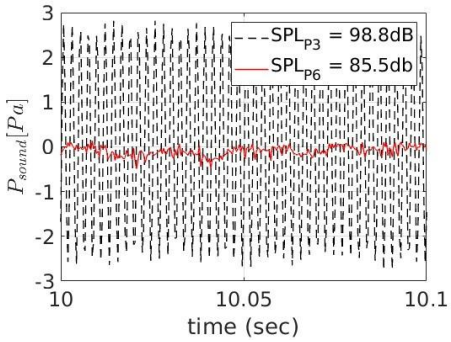

(c) Point 3 and point 6

Fig. 5. Sound pressure fluctuations measured around the sound source of 400 Hz (point 1 to point 6)

The variations in SPL levels indicate that the measured sound levels are not perfectly uniform across different positions. Position 3 exhibits the highest SPL at 98.8 dB, while Position 6 records the lowest SPL at 85.5 dB. However, positions that are symmetrically located, such as Position 1 and Position 4 or Position 2 and Position 5, have relatively close SPL values, which suggests a degree of uniformity in sound distribution.

Examining the waveform characteristics, the pressure fluctuations at different positions do not appear completely identical, although their general trends are similar. At Position 6, the waveform amplitude is noticeably lower compared to Position 3, suggesting a reduction in acoustic energy in that region. This could be attributed to either increased absorption effects in the anechoic chamber or variations in wave propagation due to spatial positioning.

An ideal anechoic wind tunnel should exhibit a uniform sound field with minimal reflections. The observed SPL variations suggest that while the chamber effectively minimizes unwanted reflections, some differences in sound distribution persist. The reduction in SPL at Position 6 compared to other positions might indicate the presence of additional absorption effects or specific positioning factors relative to the noise source.

In conclusion, the anechoic wind tunnel demonstrates a reasonably high level of sound uniformity, although it is not perfect. The SPL values across different measurement positions remain within a reasonable range, with some variation likely due to the chamber's acoustic absorption characteristics. While the chamber effectively suppresses reflections, there are still spatial

inconsistencies that influence the sound distribution. While these variations are typical, they can be mitigated through improved acoustic panelling or refined chamber geometry, as suggested by Abdel Aziz *et al.,* [23].

Figure 6 presents the Power Spectrum Density (PSD) of the 400 Hz noise source measured at six different positions inside the anechoic wind tunnel. Each subfigure compares the frequency spectrum at two positions. In Figure 6(a), the PSD is compared between Position 1 and Position 4. Similarly, Figure 6(b) compares Position 2 and Position 5, while Figure 6(c) shows the PSD for Position 3 and Position 6.

The PSD results provide insight into the uniformity of the sound field within the anechoic wind tunnel. Ideally, an anechoic environment should ensure a consistent and uniform acoustic field with minimal reflections and spatial variations. The spectra across different measurement positions exhibit similar overall trends, particularly in the low-frequency range, suggesting that the chamber effectively minimizes external influences and reflections. However, some discrepancies between corresponding positions can be observed.

In the low-frequency region, the sound pressure levels remain relatively high before gradually decreasing as the frequency increases. This trend is consistent across all measurement points, which confirms the controlled dissipation of acoustic energy. However, noticeable differences exist in the PSD magnitude at certain positions. For instance, Position 3 exhibits a higher overall SPL compared to Position 6, indicating that the sound distribution is not entirely uniform. Similarly, small variations between symmetric points such as Positions 1 and 4 or Positions 2 and 5 suggest that the acoustic absorption within the chamber may not be perfectly homogeneous.

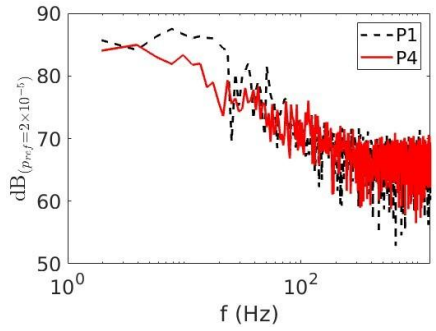

(a) Point 1 and point 4

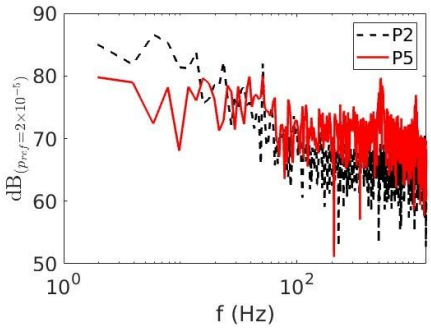

(b) Point 2 and point 5

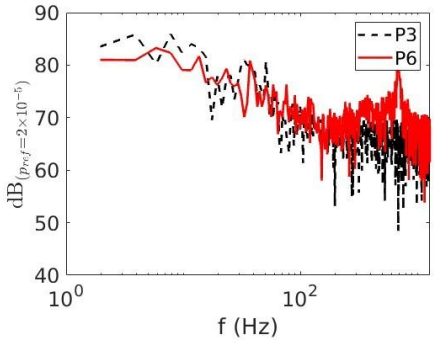

(c) Point 3 and point 6

Fig. 6. Power spectrum density of 400 Hz noise source

These discrepancies may arise due to spatial differences in sound propagation, minor asymmetries in the chamber's acoustic treatment or slight variations in microphone placement. Despite these variations, the overall similarity in spectral characteristics indicates that the anechoic wind tunnel performs well in maintaining a largely uniform sound field. The reduction in sound

energy at higher frequencies is consistent across all measurement points, further reinforcing the chamber's effectiveness in preventing unwanted reflections.

In conclusion, the anechoic wind tunnel demonstrates a reasonable degree of sound uniformity, with spectral trends remaining largely consistent across measurement points. However, some spatial variations in SPL levels indicate minor non-uniformities in the acoustic environment. While these variations do not significantly affect the chamber's overall performance, further optimization in sound absorption distribution could enhance the uniformity of the sound field inside the test section.

Figure 7 presents a polar plot of the Sound Pressure Level (SPL) measured in decibels (dB) at one-meter distance around the sound source, which is located at the centre of the anechoic chamber. The angular position represents the azimuthal angle around the source, with the SPL values recorded at multiple angles, spanning from 0 to 360 .

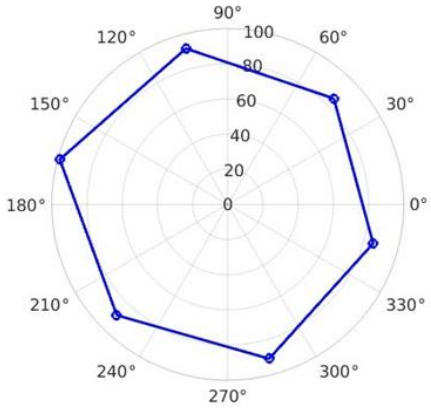

Fig. 7. Sound pressure level (dB) measured one meter around the sound sources located at the centre of the anechoic chamber

From the plot, it is evident that the sound pressure distribution around the source is not perfectly uniform, with SPL values fluctuating between approximately 75 dB and 100 dB at different angular positions. Notably, higher SPL values are observed near the angles of 90 and 120 , suggesting potential localized reflections or directional tendencies of the sound source. Conversely, the lower SPL values near 270 could indicate areas of sound energy absorption or directional noise dissipation.

This pattern reflects the acoustic behaviour of the anechoic chamber, highlighting its effectiveness in mitigating sound reflections and reverberations. The non-uniform distribution is expected due to the imperfect source directivity and the chamber's geometry, which may influence sound propagation. In comparison to other small-scale anechoic wind tunnels, such as those described by Liu *et al.,* [24] and Yang *et al.,* [25], this figure indicates that while the chamber performs adequately at reducing sound reflections, certain angular positions may experience slightly higher sound levels. This might be attributed to design factors such as the placement of acoustic materials, source positioning or chamber dimensions.

The performance of this chamber can be benchmarked against ISO 3745, which specifies the criteria for sound measurement in anechoic and semi- anechoic rooms. According to this standard, variations in SPL within a chamber should be minimized to ensure uniform sound dissipation, particularly in the regions near the sound source. By comparison, the measured SPL fluctuations seen in this figure are within a reasonable range, although further optimization may be required to achieve more uniform sound distribution across all angles.

3.2 Aerodynamic Noise Measurement

Figure 8 presents the sound spectrum density for aerodynamic noise measured at three different flow speeds: 15 m/s, 20 m/s and 25 m/s. The spectral characteristics of the noise are analysed across a wide frequency range, with each speed represented by a distinct colour. Additionally, trend lines are included to highlight the overall behaviour of the high-frequency components.

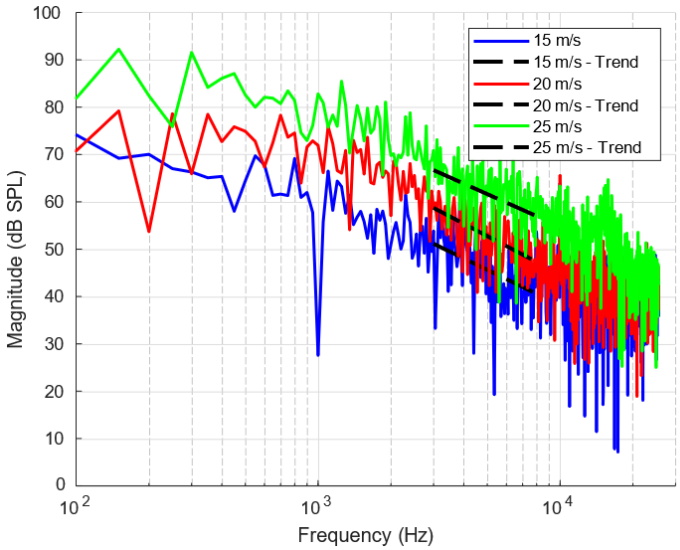

Fig. 8. Sound spectrum density for aerodynamic noise at three different speeds

The results demonstrate a clear dependence of the noise spectrum on flow velocity. At lower frequencies, the spectral levels remain relatively high across all speeds, gradually decreasing as the frequency increases. This trend is consistent with aerodynamic noise characteristics, where lower-frequency components tend to dominate due to large-scale turbulence structures, while higher-frequency noise components are generated by smaller turbulent eddies and shear-layer interactions.

A comparison of different speed cases reveals that increasing the flow velocity leads to an overall increase in sound pressure levels across the entire frequency range. The 25 m/s case exhibits the highest spectral levels, followed by the 20 m/s and 15 m/s cases. This behaviour aligns with theoretical expectations, as aerodynamic noise typically scales with flow speed, often following a power law relationship, such as SPL $\propto U^n$, where U is the flow velocity and n is an empirical exponent that varies depending on the noise source mechanism.

The presence of trend lines further clarifies the spectral decay behaviour at high frequencies. The slopes of these trend lines indicate that while all cases experience attenuation at higher frequencies, the rate of decay remains similar across different speeds. This suggests that while increasing velocity leads to higher overall noise levels, the spectral shape remains largely consistent, implying that the dominant aerodynamic noise mechanisms do not significantly change with velocity within this range.

Figure 9 presents the power-law relationship between wind speed and aerodynamic noise, illustrating how sound pressure scales with velocity. The measured data follows a power-law trend given by:

$$P \propto U^{2.91} \tag{2}$$

where P represents the sound pressure and U is the flow velocity. The exponent n = 2.91 is notably lower than the values typically associated with aerodynamic noise generated by turbulent boundary layers or jet flows. Classical aeroacoustic theory suggests that purely aerodynamic noise mechanisms, such as trailing edge noise from turbulent boundary layers, generally scale with an exponent of approximately n = 4 to 5. Jet noise, following Lighthill's acoustic analogy, exhibits even steeper scaling, with an exponent of n = 7 to 8. However, the observed exponent in this study falls within the range of n ≈ 2 to 3, which is characteristic of noise dominated by structural vibrations or mechanical sources.

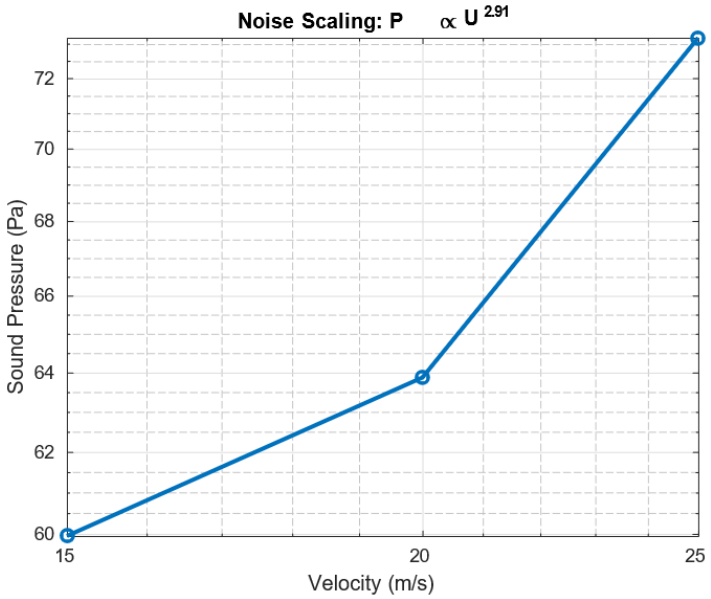

Fig. 9. Power of law for the effect of wind speed with aerodynamic noise

The relatively low scaling exponent suggests that the dominant noise source in the wind tunnel is not purely aerodynamic but is influenced by mechanical vibrations and structural noise. Potential contributors include fan and motor-induced vibrations propagating through the wind tunnel structure, resonance effects within the duct or diffuser system and oscillations of the tunnel's panels or mounting supports. These structural elements may amplify certain noise components, leading to the observed power-law relationship. To mitigate these effects, future designs could incorporate vibration isolation mounts for the fan and motor, add constrained-layer damping materials to critical panels and optimize duct geometry to reduce flow-induced resonances. If the primary noise source were dipole-type aerodynamic noise, typically associated with fluctuating surface pressures such as trailing edge noise, the expected exponent would be closer to n = 4. The discrepancy indicates that structural interactions are likely a significant factor in the measured noise levels.

The findings from Figure 9 suggest that improvements in the wind tunnel's structural design and noise control strategies could reduce unwanted mechanical noise contributions. Enhancing vibration isolation, implementing additional damping materials or optimizing the aerodynamic design of the tunnel could help minimize these effects and provide a clearer assessment of true aerodynamic noise characteristics. A more detailed analysis, such as structural modal testing or noise source separation techniques, could further clarify the contributions of different noise sources.

In conclusion, the power-law scaling observed in this study indicates that structural vibrations and mechanical noise, rather than purely aerodynamic sources, play a significant role in the overall

noise levels. This finding underscores the importance of addressing structural factors when analysing aerodynamic noise in wind tunnel environments.

3.3 Noise Frequency Range in Anechoic Wind Tunnel Design

For airfoil aeroacoustic investigations, the frequency range of the anechoic wind tunnel must be carefully designed to capture the dominant noise-generating mechanisms. The appropriate frequency range depends on the flow conditions, airfoil dimensions and the specific aeroacoustic phenomena under investigation.

Based on research and industry standards, a typical anechoic wind tunnel designed for airfoil noise studies should provide anechoic performance in the range of:

$$f_{min} \approx 100 \text{ Hz} \quad \text{to} \quad f_{max} \approx 10 \text{ kHz} \tag{3}$$

This ensures that both low-frequency airfoil self-noise originating from boundary layers and flow interactions and high-frequency turbulence-related noise, such as vortex shedding and trailing-edge noise, are accurately measured. The required frequency range is influenced by different airfoil noise sources:

i. Low-Frequency Noise (100 Hz – 500 Hz): This range typically includes airfoil tonal noise from laminar boundary-layer vortex shedding. If the flow remains mostly attached, coherent vortex shedding may occur at well-defined tonal frequencies within this range.
ii. Mid-Frequency Noise (500 Hz – 3 kHz): This region is crucial for studying trailing-edge noise, which arises from turbulent boundary- layer interactions with the airfoil's sharp edge. Most trailing-edge noise falls within this range, particularly for moderate Reynolds numbers in the order of 105 − 106.
iii. High-Frequency Noise (3 kHz – 10 kHz and above): This range is important for turbulent-boundary-layer noise and leading-edge noise caused by interactions with upstream turbulence or impinging gusts. High-speed flows or small-scale turbulence contribute significantly to noise levels in this region.

Figure 10 presents the noise frequency sensitivity range, illustrating the variation in sound pressure levels for different frequency components. The data includes measurements at three representative frequencies: 500 Hz, 1500 Hz and 10,000 Hz, each corresponding to different noise sources relevant to aeroacoustic studies. The figure provides insights into the effectiveness of the anechoic wind tunnel in absorbing unwanted reflections and ensuring accurate aeroacoustic measurements across a broad spectrum.

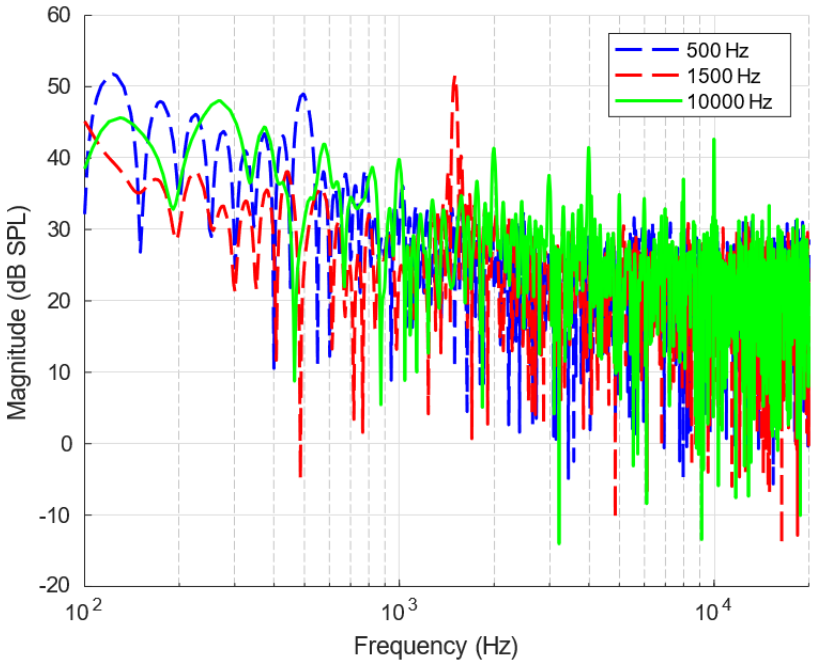

Fig. 10. Noise frequency sensitivity range

The 500 Hz case (dotted blue line) represents low-frequency aerodynamic noise, which is often associated with large-scale turbulence structures, vortex shedding and boundary-layer interactions. The fluctuations observed in this range suggest that while the anechoic wind tunnel effectively suppresses some reflections, minor variations indicate that low-frequency absorption may require further optimization. Achieving good anechoic performance at low frequencies is inherently challenging due to longer acoustic wavelengths, which require deeper acoustic wedges or hybrid absorption techniques.

The 1500 Hz case (dashed red line) corresponds to mid-frequency noise, a crucial range for trailing-edge noise and turbulent boundary-layer interactions. The relatively stable spectral behaviour in this region suggests that the wind tunnel provides sufficient absorption, allowing for accurate measurement of airfoil self-noise and other mid-frequency aeroacoustic phenomena. The reduced spectral fluctuations indicate that mid-frequency reflections are well- controlled, confirming the chamber's effectiveness in minimizing interference from unwanted noise sources.

The 10,000 Hz case (solid green line) captures high-frequency noise, typically generated by small-scale turbulence, shear-layer instabilities and leading- edge interactions. The spectral uniformity at this frequency confirms that the anechoic chamber provides excellent high-frequency absorption, effectively eliminating unwanted reflections. The smooth trend in the high-frequency range indicates that the wind tunnel meets the necessary free-field conditions, making it highly suitable for precise aeroacoustic investigations in this spectral region.

The results from Figure 10 highlight the overall quality of the designed anechoic wind tunnel for aeroacoustic studies. The chamber performs exceptionally well in the mid- and high-frequency ranges, ensuring reliable measurements of turbulence-induced noise, vortex interactions and shear-layer instabilities. However, low-frequency noise exhibits some fluctuations, suggesting that further refinements in acoustic treatment such as enhanced wall damping, deeper absorbers or alternative hybrid suppression methods—may be beneficial in reducing standing waves and residual reflections.

In conclusion, Figure 10 validates the effectiveness of the anechoic wind tunnel for aeroacoustic research. The chamber demonstrates strong anechoic performance at mid-to-high frequencies, making it well-suited for studies on airfoil noise, turbulence-generated sound and aerodynamic

instabilities. While low-frequency absorption could be further improved, the current setup provides a high-quality anechoic environment for detailed aeroacoustic investigations.

4. Conclusions

This study presents the design and validation of a small open anechoic wind tunnel for aeroacoustic testing. The results indicate that the chamber effectively minimizes reflections and maintains a controlled acoustic environment. While slight variations in sound pressure levels exist across measurement positions, the chamber provides sufficient uniformity for reliable noise measurements. The power spectrum density analysis confirms that the tunnel suppresses external noise and maintains consistent spectral trends, particularly at mid- to-high frequencies. However, minor discrepancies in low-frequency absorption suggest the need for further optimization in acoustic treatment. Aerodynamic noise measurements reveal a power-law scaling exponent of 2.91, indicating a contribution from structural vibrations, which could be mitigated through improved vibration isolation. The frequency response analysis highlights strong performance above 500 Hz, making the tunnel well-suited for studying trailing-edge noise, boundary- layer interactions and turbulence-induced noise. While low-frequency absorption remains a challenge, the overall results validate the chamber's effectiveness for aeroacoustic research. Further improvements in structural design and acoustic treatment could enhance its performance for broader applications in aerodynamic noise studies.

Acknowledgement
The authors acknowledge the financial support by Universiti Teknologi Malaysia under Fundamental Research Grant, reference number PY/2023/01864 and cost centre number Q.K130000.3810.22H98.

References
[1] Giardino, Frank and Joana Rocha. "Design and characterization of a high-speed subsonic aeroacoustic wind tunnel." *Journal of Aircraft* 56, no. 1 (2019): 108-120. https://doi.org/10.2514/1.C035113
[2] Yi, Wei, Peng Zhou, Yi Fang, Jingwen Guo, Siyang Zhong, Xin Zhang, Xun Huang, Guocheng Zhou and Bao Chen. "Design and characterization of a multifunctional low-speed anechoic wind tunnel at HKUST." *Aerospace Science and Technology* 115 (2021): 106814. https://doi.org/10.1016/j.ast.2021.106814
[3] Auhl, Richard R., Dennis K. McLaughlin and Philip J. Morris. "Design, assembly and testing of an upgraded aeroacoustics wind tunnel facility." *International Journal of Aeroacoustics* 23, no. 3-4 (2024): 285-298. https://doi.org/10.1177/1475472X241230650
[4] ISO, BSSN. "3745, Acoustics—Determination of Sound Power Levels and Sound Energy Levels of Noise Sources Using Sound Pressure—Precision Methods for Anechoic Rooms and Hemi-Anechoic Room." *International Standard Organization* (2012).
[5] ISO, BSSN. "26101:2012, Acoustics – Test methods for qualification of free-field environments." *International Organization for Standardization,* (2012).
[6] Russo, Mladen, Luka Kraljević, Maja Stella and Marjan Sikora. "Acoustic performance analysis of anechoic chambers based on ISO 3745 and ISO 26101: standards comparison and performance analysis of the anechoic chamber at the University of Split." In *Proc. Euronoise*, pp. 1-6. 2018.
[7] de Santana, Leandro D., Martinus P. Sanders, Cornelis H. Venner and Harry W. Hoeijmakers. "The UTwente aeroacoustic wind tunnel upgrade." In *2018 AIAA/CEAS Aeroacoustics Conference*, p. 3136. 2018. https://doi.org/10.2514/6.2018-3136
[8] Spalt, Taylor B., Thomas F. Brooks, Christopher J. Bahr, Lawrence Becker, Daniel J. Stead and Gerald E. Plassman. "Calibrations of the NASA Langley 14-by 22-Foot Subsonic Tunnel in Acoustic Configuration." In *20th AIAA/CEAS Aeroacoustics Conference*, p. 2344. 2014. https://doi.org/10.2514/6.2014-2344
[9] Merino-Martínez, Roberto, Alejandro Rubio Carpio, Lourenço Tércio Lima Pereira, Steve van Herk, Francesco Avallone, Daniele Ragni and Marios Kotsonis. "Aeroacoustic design and characterization of the 3D-printed, open-

jet, anechoic wind tunnel of Delft University of Technology." *Applied Acoustics* 170 (2020): 107504. https://doi.org/10.1016/j.apacoust.2020.107504

[10] STANDARD, BRITISH and BSEN ISO. "Acoustics ƒ Measurement of sound absorption in a reverberation room." (2003).

[11] Vercammen, Martijn. *On the revision of ISO 354, measurement of the sound absorption in the reverberation room*. Universitätsbibliothek der RWTH Aachen, 2019.

[12] Othman, Nor'Azizi and Abdul Rahman, Nurul Ashmira. "The Effects of Acoustic Absorbing Materials in Noise Reduction of Exhaust Muffler System." *Journal of Advanced Research Design*, 76(1), (2024): 1–13.

[13] International Electrotechnical Commission *et al.,* "Electroacoustics—sound level meters—part 1." *Specifications (IEC 61672-1). Geneva, Switzerland*, (2013).

[14] Takahashi, Hironobu, Keisuke Yamada and Ryuzo Horiuchi. "Physical Quantities of Sound and Expanding Demands for Noise Measurement." In *Handbook of Metrology and Applications*, pp. 1527-1569. Singapore: Springer Nature Singapore, 2023. https://doi.org/10.1007/978-981-99-2074-7_85

[15] Amaral, F. R., JC Serrano Rico, C. S. Bresci, M. M. Beraldo, V. B. Victorino, E. M. Gennaro and M. A. F. Medeiros. "The low acoustic noise and turbulence wind tunnel of the University of Sao Paulo." *The Aeronautical Journal* 126, no. 1297 (2022): 500-532. https://doi.org/10.1017/aer.2021.80

[16] Koop, Lars and Klaus Ehrenfried. "Microphone-array processing for wind-tunnel measurements with strong background noise." In *14th AIAA/CEAS Aeroacoustics Conference (29th AIAA Aeroacoustics Conference)*, p. 2907. 2008. https://doi.org/10.2514/6.2008-2907

[17] Hanson, Carl Elmer. "The design, development and construction of a low-noise, low-turbulence wind tunnel." PhD diss., Massachusetts Institute of Technology, 1967.

[18] Devenport, William J., Ricardo A. Burdisso, Aurelien Borgoltz, Patricio A. Ravetta, Matthew F. Barone, Kenneth A. Brown and Michael A. Morton. "The Kevlar-walled anechoic wind tunnel." *Journal of Sound and Vibration* 332, no. 17 (2013): 3971-3991. https://doi.org/10.1016/j.jsv.2013.02.043

[19] Okoronkwo, M. K., R. Alsaif, R. Haklander, S. Baba, J. M. Eburn, Z. Lu, N. Arafa, O. Stalnov, A. Ekmekci and P. Lavoie. "Design and characterization of the university of Toronto hybrid anechoic wind tunnel." *Applied Acoustics* 228 (2025): 110294. https://doi.org/10.1016/j.apacoust.2024.110294

[20] Mathew, Jose, Chris Bahr, Mark Sheplak, Bruce Carroll and Louis N. Cattafesta. "Characterization of an anechoic wind tunnel facility." In *ASME International Mechanical Engineering Congress and Exposition*, vol. 42258, pp. 281-285. 2005. https://doi.org/10.1115/IMECE2005-81737

[21] Doolan, C. J., Danielle Moreau, Manuj Awasthi and Chaoyang Jiang. "The UNSW anechoic wind tunnel." *Proceedings of WESPAC 2018* (2018).

[22] Robinson, David P. and James Tingay. "Comparison study of the performance of smartphone-based sound level meter apps, with and without the application of a 1/2." In *INTER-NOISE and NOISE-CON Congress and Conference Proceedings*, vol. 249, no. 4, pp. 3815-3824. Institute of Noise Control Engineering, 2014.

[23] Abdel Aziz, Salem S., Essam B. Moustafa and Abdel-Halim Saber Salem Said. "Experimental Investigation of the Flow, Noise and Vibration Effect on the Construction and Design of Low-Speed Wind Tunnel Structure." *Machines* 11, no. 3 (2023): 360. https://doi.org/10.3390/machines11030360

[24] Liu, Peiqing, Yu Xing, Hao Guo and Ling Li. "Design and performance of a small-scale aeroacoustic wind tunnel." *Applied Acoustics* 116 (2017): 65-69. https://doi.org/10.1016/j.apacoust.2016.09.014

[25] Yang, Yannian, Yu Liu, Rui Liu, Chao Shen, Pikai Zhang, Renke Wei, Xiaomin Liu and Pengwei Xu. "Design, validation and benchmark tests of the aeroacoustic wind tunnel in SUSTech." *Applied Acoustics* 175 (2021): 107847. https://doi.org/10.1016/j.apacoust.2020.107847